Check for updates

European Journal of Inflammation

Original Research Article

Implementation of an automated inclusion system for the histological analysis of murine tissue samples: A feasibility study in DSS-induced chronic colitis

European Journal of Inflammation
Volume 16: 1–12
© The Author(s) 2018
Reprints and permissions:
sagepub.co.uk/journalsPermissions.nav
DOI: 10.1177/2058739218776883
journals.sagepub.com/home/eji
SAGE

Fulvia Milena Cribiù,[1] Claudia Burrello,[2] Giulia Ercoli,[1] Federica Garavaglia,[2] Vincenzo Villanacci,[3] Flavio Caprioli,[4,5] Silvano Bosari[1] and Federica Facciotti[2]

Abstract

Animal models are powerful tools to expand our understanding of human diseases. Histopathological evaluation of murine experimental models is often required to support further research; thus, a more rigorous evaluation of murine histological samples is strongly advocated. Indeed, the overall quality of tissue sections is critical to draw reliable and accurate conclusions. As several methodological variables may reduce the reliability of the pathological analysis, a standardization of the procedural steps required for the processing of histological murine tissues is advisable. Here, we describe a method to standardize the technical procedure from the initial preparation to the paraffin embedding of murine samples. Specifically, we have implemented an automated inclusion system, that is, the SAKURA Tissue-Tek inclusion instrument, which is routinely used for paraffin inclusion of human samples, to process murine specimens of intestinal inflammation. Colitis severity was assessed in chronically Dextran Sodium Sulphate (DSS)–treated mice by cytofluorimetric analysis of colonic cellular infiltrates, expression of inflammatory genes and histopathological analysis of tissue samples, comparing manual and automated tissue preparation systems. We here conclude that implementation of this technique can significantly increase the quality and the reliability of histopathological examination of murine tissues.

Keywords

automation, chronic colitis, histopathological analysis, murine models

Date received: 26 September 2017; accepted: 20 April 2018

Introduction

In the last decades, animal models have been increasingly utilized as a tool to expand our understanding of the pathogenesis of human diseases.[1,2] During the experimental process, researchers are often faced with the need to perform detailed histopathological analyses to assess the severity of a disease, the effect of a treatment, or to demonstrate, in a specific experimental setting, a variation in the architecture of a tissue or of its infiltration by immune cells.[3]

The increasing complexity of translational research often implies the concomitant evaluation of human and murine samples.[4] A detailed histopathological

[1]Pathology Unit, Fondazione IRCCS Cà Granda, Ospedale Policlinico di Milano, Milan, Italy
[2]Department of Experimental Oncology, European Institute of Oncology (IEO), Milan, Italy
[3]Pediatrics Clinic, Department of Clinical and Experimental Sciences, Spedali Civili, University of Brescia, Brescia, Italy
[4]Gastroenterology and Endoscopy Unit, Fondazione IRCCS Cà Granda, Ospedale Maggiore Policlinico, Milan, Italy
[5]Department of Pathophysiology and Transplantation, Università degli Studi di Milano, Milan, Italy

Corresponding author:
Claudia Burrello, Department of Experimental Oncology, European Institute of Oncology (IEO), Via Adamello 16, 20139 Milan, Italy.
Email: Claudia.burrello@ieo.it

Creative Commons Non Commercial CC BY-NC: This article is distributed under the terms of the Creative Commons Attribution-NonCommercial 4.0 License (http://www.creativecommons.org/licenses/by-nc/4.0/) which permits non-commercial use, reproduction and distribution of the work without further permission provided the original work is attributed as specified on the SAGE and Open Access pages (https://us.sagepub.com/en-us/nam/open-access-at-sage).

analysis of murine experimental models is therefore becoming straightforward to support further research, and extrapolation of data from murine models represents a common way to proceed to understand human pathologies.[5]

Nevertheless, while human samples are processed and scored by histopathology core facilities and experienced human pathologists through precise histopathological criteria, murine tissues are usually fixed, included and analysed by researchers with limited experience in histopathology and histopathological methods. Conversely, few human pathologists have the possibility to directly contribute to ameliorate the quality of the analysis of murine experimental samples.

Fixation, macroscopic sectioning, processing, paraffin embedding and inclusion of the samples play a major role in section quality,[6] which is an essential prerequisite to draw confident and precise diagnostic conclusions.[7]

Manual inclusion of the samples and, to a lesser extent, manual microtomy cutting and staining contribute to lower the quality of the analysis. Unfortunately, the whole process of murine tissue preparation is based on protocols that vary from laboratory to laboratory and in part depend on those variables linked to the operator manual skills. In order to improve the standardization of murine tissue preparations, we here propose to implement an automated protocol of inclusion[8] that is commonly used for human samples, also for the histological analysis of murine tissues, which was compared to the manual procedure. As a practical example of the feasibility of the method, a murine model of intestinal inflammation has been analysed.

Materials and methods

Mice

C57Bl/6 mice (8–10 weeks of age) were purchased from Charles River and housed at the animal facility of European Institute of Oncology (IEO). Animal procedures were approved by the Italian Ministry of Health (Auth. 127/15). Mice were administered three rounds of 2.5% Dextran Sodium Sulphate (DSS; TdB Consultancy, Uppsala, Sweden) in drinking water for 1 week interspaced with 2 weeks of rest in between. Optimal DSS concentration was determined via preliminary titration experiments, taking into consideration the lot number, the mouse strain, age and gender as well as environmental factors related to the rearing conditions of the animal facility.[9] Mice were sacrificed at day 63. Colon were removed and colon length was measured with a caliper and subsequently divided in portions to be fixed in 10% formalin for histology, snap frozen for RNA analyses and the rest for lamina propria mononuclear cells' (LPMCs) extraction for immunophenotyping.

Murine LPMCs isolation

For the isolation of LPMCs from mouse colons, Peyer's patches were removed, lamina propria lymphocytes (LPLs) were isolated via incubation with 5 mM ethylenediaminetetraacetic acid (EDTA) at 37°C for 30 min followed by further digestion with collagenase IV and DNase at 37°C for 1 h. Cells were then further separated with a Percoll gradient.

Flow cytometry

Murine LPL were stained with anti-CD45.2 (104), anti-CD11b (M1/70), anti-Ly6G (1A8), anti-CD11c (N418), anti-CD3 (17A2), anti-CD4 (GK1.5) and anti-CD8 (53-6.7), all purchased from BD, United States, or BioLegend, United States).

Samples were analysed on a FACSCanto flow cytometer (BD), gated to exclude nonviable cells on the basis of light scatter and, in some experiments, by incorporation of Aqua Dye according to manufacturer's protocol (Invitrogen, United States). Data were analysed using FlowJo software (BD).

mRNA quantification by quantitative polymerase chain reaction

Total RNA from murine colonic tissues was isolated using TRIZOL and Quick-RNA MiniPrep (ZymoResearch, United States) according to manufacturer's instructions. cDNAs were generated from 1 µg of total RNA with reverse transcription kit (Promega, United States). Tumor necrosis factor (TNF) and CXCL10 expression levels were evaluated by quantitative polymerase chain reaction (qPCR) and normalized to L32 expression. Primer sequences used were as follows: TNF 5′-TCTTCTCATTCCTGCTTGTGG-3′ and 5′-CACTTGGTGGTTTGCTACGA-3′; CXCL10 5′-CGCTGCAACTGCATCCATATCG-3′ and 5′-CCGGATTCAGACATCTCTGCTC-3′.

Patients

Pictures of haematoxylin and eosin (H&E), Azan-Mallory staining and immunohistochemistry (IHC) were obtained from the surgical specimen of a Crohn's disease patient undergoing ileocolonic resection for stricturing disease at the Policlinico Hospital Milan. The Ethical Committee of Policlinico Hospital Milan gave approval, and informed consent was obtained. Immediately after bowel resection, unfixed surgical specimens were transferred to the Pathology Department, where a single experienced pathologist (M.C.) sampled the tissue to obtain a complete full-thickness section.

Tissue processing (mouse and human samples)

Tissue processing was performed with a LEICA PELORIS processor (Leica Biosystems, Germany) that uses a series of graded alcohols for dehydration and xylene for cleaning before paraffin impregnation. The whole process lasts a total of 13 h and 28 min. The series was as follows: formalin, 120 min 45°C; distilled water, 2 min 45°C; 2× 95% EtOH, 60 min 45°C, 3× absolute ethanol (EtOH), 60 min 45°C; 3× xylene, 60 min 45°C and 2× Paraffin, 60 min 65°C. Murine samples were either included by using a manual procedure or an automated system (SAKURA Tissue-Tek, Torrance, CA, USA), as further detailed in the 'Results' section.

H&E staining

The H&E stain was performed by staining the specimen with Harris' haematoxylin (aluminium potassium sulphate, haematoxylin, absolute alcohol, mercuric oxide and glacial acetic acid) followed by 1% acid alcohol and, subsequently, 1% eosin. Snapshots of histology were taken using an Aperio CS2 microscope with a scanning resolution of 50,000 pixels per inch (0.5 µm per pixel with 20× objective) and 0.25 µm per pixel when scanning at 40× with 2× magnification changer.

IHC

For IHC analysis, sections were first deparaffinized. Murine antigens retrieval was performed by immersing the sections in 10 mM citrate buffer (pH 6.5) and heating them twice in a microwave oven (95°C) for 5 min each time. Endogenous peroxidase activity was blocked by incubation with 1% hydrogen peroxide in distilled water for 10 min. Murine sections were incubated with polyclonal anti-CD3 (clone F7.2.38, rabbit, DAKO, United States) and then with secondary antibodies.

Human sections were incubated with anti-CD3 (DAKO, clone 2GV6, rabbit) and then with secondary antibodies.

Heidenhain-Azan-Mallory trichrome staining

From each tissue sample, one section was stained for collagen deposition and fibrosis analysis by using Azan-Mallory trichrome stain for standard method. In this method, three different dyes are used: carbol fuchsin for nuclear staining, Orange G for cytoplasm and aniline blue for the specific collagen staining. The protocol used was the S-Trichrome (v1.00.0111) from Ventana Medical System (United States), barcode 3011.

Statistics

Statistical significance was determined using Wilcoxon matched-pairs signed rank t test not parametric and not assuming Gaussian distribution. $P<0.05$ (*), $P<0.005$ (**) and $P<0.0005$ (***) were regarded as statistically significant.

Results

Experimental chronic colitis is characterized by colonic immune cell infiltration and upregulation of inflammatory genes

Chronic colitis caused by repeated administration of DSS in the drinking water (Figure 1(a)) is a murine model of intestinal inflammation closely resembling human inflammatory bowel disease (IBD). DSS-treated animals exhibit signs of intestinal inflammation, including weight loss, loose stool or diarrhoea, and shortening of the colon (Figure 1(b)).

To confirm the presence of active intestinal inflammation, mRNA levels of pro-inflammatory mediators were evaluated in colonic tissue fragments. Tumour necrosis factor (TNF) and the chemokine CXCL10 (Figure 1(c)) were significantly increased in DSS chronic colitis with respect to untreated controls. Flow cytometric analysis of immune cells extracted from colonic mucosa during intestinal inflammation confirmed an increased infiltration of inflammatory cells, including Ly6G+

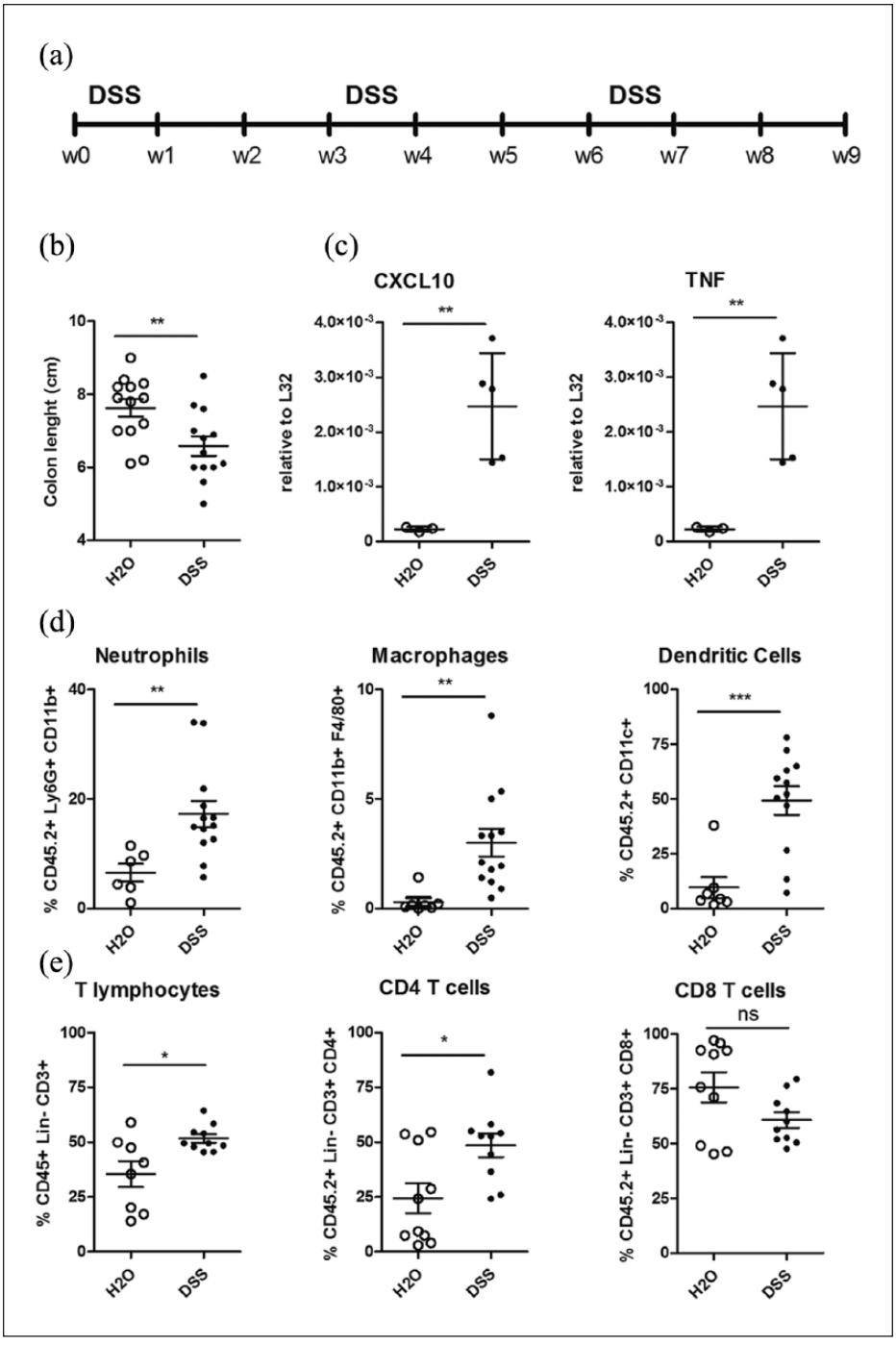

Figure 1. Chronic intestinal inflammation in DSS-treated mice. (a) Experimental design of chronic DSS treatment. (b) Colon length measurement. (c) Gene expression analysis of pro-inflammatory cytokines (CXCL10 and TNF) in inflamed colon tissue (closed symbols, n = 5) as compared to controls (open symbols, n = 5). (d, e) Flow cytometric analyses of colonic lamina propria cells in inflamed colon (closed symbols, n = 12) as compared to control mice (open symbols, n = 6). (d) CD11b+Ly6G+ neutrophils (left panel), CD11b+F4/80+ macrophages (middle panel) and CD11c+ dendritic cells (right panel) infiltration in control (open symbols) and DSS-treated mice (closed symbols). (e) Total T cell infiltration (left panel), CD4+ (middle panel) and CD8+ T cells (right panel) in control (open symbols, n = 9) and DSS-treated (closed symbols, n = 9) mice. Statistical significance was calculated using Wilcoxon matched-pairs signed rank t test. $^{*}P < 0.05$; $^{**}P < 0.005$; $^{***}P < 0.0005$.

CD11b+ neutrophils, CD11b+F40/80+ macrophages and CD11c+ dendritic cells (Figure 1(d)), and of T lymphocytes (Figure 1(e)), especially CD4+ T cells.

Taken together, these data confirm at the immunological and molecular level that the animals in this experimental setting are undergoing an

intestinal inflammatory response as a consequence of experimental DSS-induced chronic colitis.

Standardization of murine tissue preparation

The quality of a histopathological examination is strongly dependent on the preparation of the tissue sample. To increase the overall quality of the staining and minimize experimental errors, we explored the possibility to apply and validate an automated method commonly used for human pathological sample examination, that is, the SAKURA Tissue-Tek system, to murine tissues.

Immediately after sacrifice, tissue specimens were immersed in a 10% neutral buffered formalin container. A fixation time, strictly ranging from 18 to 24 h, allowed all tissues to be uniformly fixed, thus increasing the subsequent tissue sectioning and staining quality.

Fixed tissue specimens were macroscopically sectioned and cut in smaller pieces to be accommodated in the histological paraffin embedding cassettes (Figure 2(a)–(c)). Closed murine colon specimens (of a length comprised from 0.6 to 1.5 cm, with a lumen diameter between 0.2 and 0.3 mm) were cut in homogeneous pieces of 0.2–0.3 mm length (Figure 2(d)) and then inserted inside the cassette (Figure 2(d)). We utilized cassettes specifically designed for tissues that require a vertical orientation or provided with a lumen. These cassettes contain a grid with extruded tips that allow the insertion of the tissue vertically and with the proper orientation, that is, with the lumen in the inner part and the wall exteriorly (Figure 2(d) and (e)). To optimize the occupation of cassette space and uniform tissue insertion in the grids for current and future analyses, three to four pieces of colon were vertically inserted in defined positions of the grid, as depicted in Figure 2(e) and (f). By doing so, all the samples were similarly included.

The cassettes were then closed (Figure 2(f)). The presence of the grids allowed the preservation of the orientation, contrary to what happens with conventional histological cassettes (Figure 2(g)–(i)).

Processing and automated embedding

After tissue processing, carried through with a LEICA PELORIS, the embedding procedure was performed with an automated embedder (Tissue-Tek AutoTEC, SAKURA, Netherlands), where a robot collects the cassettes and dispenses the correct amount of paraffin. At the end of the procedure, micrometer sections were cut form each block using an automated LEICA Rotary microtome (RM2255), and the slides were prepared as in Figure 2(l) and (m) for further analysis. Paraffin blocks were cut until the microtome reached the grid. When the grid was cut off, a first 3-nm-thick section was collected on the top part of a glass slide and a second one of the same thickness was cut after 50 nm and collected on the lower part of the slide. In this way, two homogeneous slices of the same tissue were collected in two distant parts of the slide to be analysed to evaluate the extent of the lesions, when present, and the changes in tissue morphology (Figure 2(l)–(n)).

Automated processing of intestinal samples generates high-quality histological images

The extent of the inflammatory response observed during experimental intestinal inflammation can be scored on the basis of an accurate analysis of histological alterations in the bowel wall. Histopathological scores were assessed according to the grading system shown in Table 1 for the same samples that were used for flow cytometric analyses and RNA quantification in Figure 1 and prepared with the automated system described in Figure 2. This scoring system evaluates the modifications of different parameters occurring upon intestinal inflammation in the entire intestinal wall, such as immune cell infiltration, epithelial changes and variation of mucosal architecture.

The H&E staining of untreated mice (Figure 3(a)) was compared to those of DSS-treated mice (Figure 3(b)–(f)). DSS-induced intestinal inflammation was characterized by a marked thickening of the muscularis mucosae (as indicated by the black bar), and a marked inflammatory infiltrate involving the entire colonic wall, up to the visceral adipose tissue, made up of lymphocytes, plasma cells and neutrophils (mucosal immune cell infiltrate, green triangle, submucosal infiltrate and oedema, light blue triangle and data not shown analysed at higher magnification). Submucosal infiltration was mainly composed by neutrophils and eosinophils (light blue triangle and data not shown analysed at higher magnification). In addition, DSS-treated mice showed colonic epithelial hyperplasia and mitoses (red

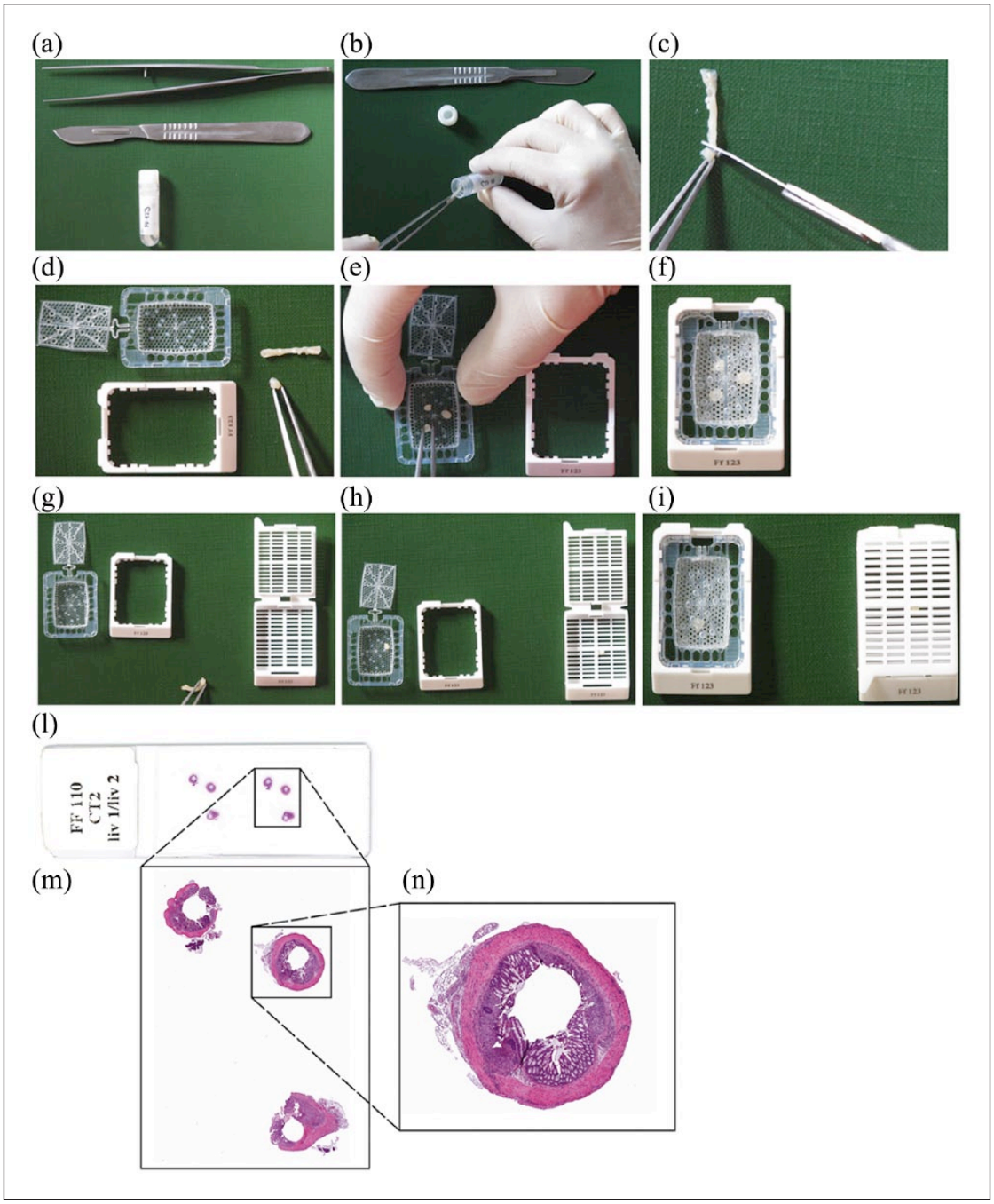

Figure 2. A standardized tissue inclusion method minimizes variability. (a) Instruments needed for tissue preparation. (b) The pathologist extracts the tissue from the vial and (c) cuts the colon in pieces of 0.2–0.3 mm. (d) Orientated Cassettes (Finetek, SAKURA, Netherlands). External cassette (white) and internal grid with extruded orientation tips. (e, f) Insertion of murine colons in the internal grids Cassettes before (e) and after (f) closing of the grids. (g–i) Comparison between insertion of colons in Orientated Cassettes (left) and Traditional Cassette (right). (g, h) Open cassettes. (i) Closed cassettes. (l) Picture of the slide after microtome cutting and H&E staining. Top part of the slide, 3 µm sections of tissue collected at 20 µm from the surface; bottom part, sections collected at 50 µm from the surface. (m, n) H&E staining to appreciate the orientation of the sample.

triangle), partial crypt loss and crypt abscesses (black triangle) and goblet cell depletion (yellow triangle).

The cumulative histological scores calculated for untreated and DSS-treated mice are shown in Figure 3(g).

Table 1. Scoring scheme for evaluation of intestinal inflammation.

Category	Criterion	Definition	Score value
Inflammatory cell infiltrate	Severity (leucocyte density of lamina propria area infiltrated in evaluated high-power field, HPF)	No infiltrate	0
		Minimal acute (<10%)	0.25
		Mild chronic (10%–25%, scattered neutrophils)	0.5
		Moderate chronic (26%–50%)	0.75
		Marked (>51%, dense infiltrate)	1
	Extent (expansion of leucocyte infiltration)	Mucosal	0.5
		Mucosal and submucosal	0.75
Epithelial changes	Hyperplasia (increase in epithelial cell numbers in longitudinal crypts, visible as crypt elongation)	No hyperplasia	0
		Minimal (<25%)	0.25
		Mild (26%–35%)	0.5
		Moderate (36%–50%, mitoses in the upper third of the crypt epithelium)	0.75
		Marked (>51%, mitoses in crypt epithelium distant from crypt base)	1
	Goblet cell loss (reduction of goblet cell numbers relative to baseline goblet cell numbers per crypt)	No loss	0
		Minimal (<25%)	0.25
		Mild (26%–35%)	0.5
		Moderate (36%–50%)	0.75
		Marked (>51%)	1
Mucosal architecture	Ulceration (epithelial defect reaching beyond muscularis mucosae)	No ulcers	0
		Ulcers	0.25
	Granulation tissue (connective tissue repair with new capillaries, surrounded by infiltrating cells and hypertrophied areas)	No granulation tissue	0
		Granulation tissue	0.25
	Mucosal thickness and crypt depth	No thickening	0
		Thickening	0.5
	Glandular rarefaction	No rarefaction	0
		Rarefaction	0.5
	Dysplasia	No dysplasia	0
		Dysplasia	0.5
		Maximum score	6

Automated processing of intestinal samples allows detection of complex events such as fibrosis in murine colons

We next evaluated the quality of IHC and collagen staining in murine colon sections of untreated (Figure 4(a)–(c)) and DSS-treated (Figure 4(d)–(f)) mice prepared with the automated inclusion system.

To evaluate whether the automated sample preparation could be used to evaluate complex phenomenon such as fibrotic tissue deposition, as observed in Crohn's disease patients, we performed Heidenhain's Azan trichromic staining on murine colonic sections (Figure 4(b) and (e)). As expected, Heidenhain's Azan staining of untreated mice documented a thin layer of extra-cellular matrix (ECM) and collagen deposition within the submucosa (Figure 4(b), depicted as blue staining). In contrast, colonic sections of DSS-treated mice showed transmural collagen deposition, including mucosa, muscularis mucosae, submucosa and muscularis propria. Extensive ECM deposition was detected in close association with immune cells infiltrating the mucosa, and several collagen fibrils could be seen within the muscularis mucosae and muscularis propria as well as interspersed between cells scattered throughout the oedematous submucosa (Figure 4(e)).

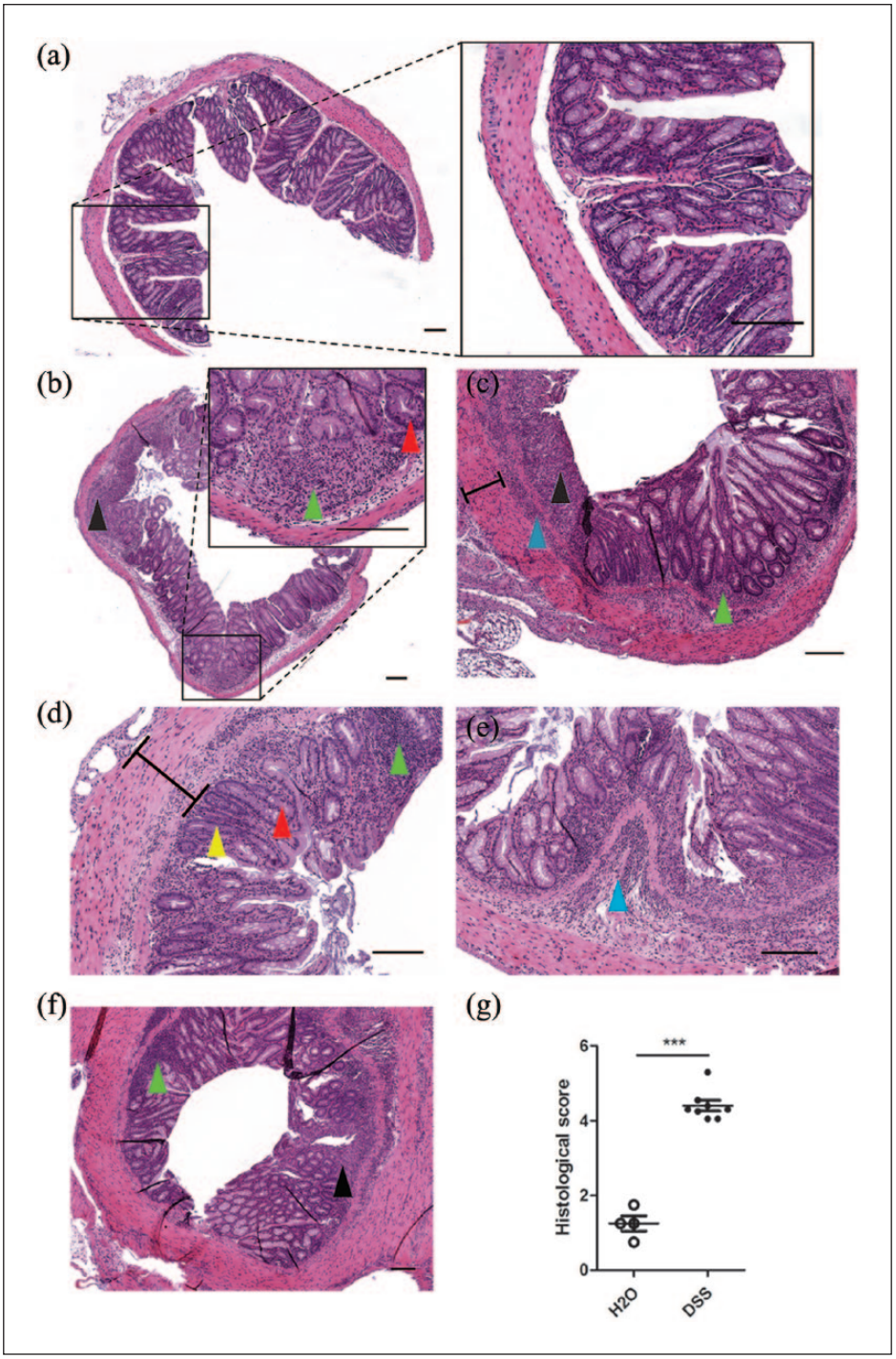

Figure 3. Histological evaluation of DSS-treated mice versus untreated controls. Examples of H&E staining from slices obtained from embedded murine colons of DSS-treated mice (a–d) and controls (e and f). Muscularis mucosa thickening, black bar; mucosal immune cell infiltrate, green triangle; submucosal immune cell infiltrate, light blue triangle; oedema, light blue triangle; colonic epithelial hyperplasia and mitosis, red triangle; crypt loss and crypt abscesses, black triangle; goblet cells rarefaction, yellow triangle. A, B, C and F 5× magnification; inserts and D, E, 10× magnification. Scale bar, 100 nm. (g) Histological cumulative score (DSS treated, n = 5; controls, n = 5).

Next, paraffin sections of untreated (Figure 4(c)) and DSS-treated (Figure 4(f)) mice were de-waxed, subjected to heat-induced epitope retrieval before incubation with antibodies to detect T cells. As observed with H&E analysis of Figures 3 and 4(d), DSS-treated mice showed immune massive

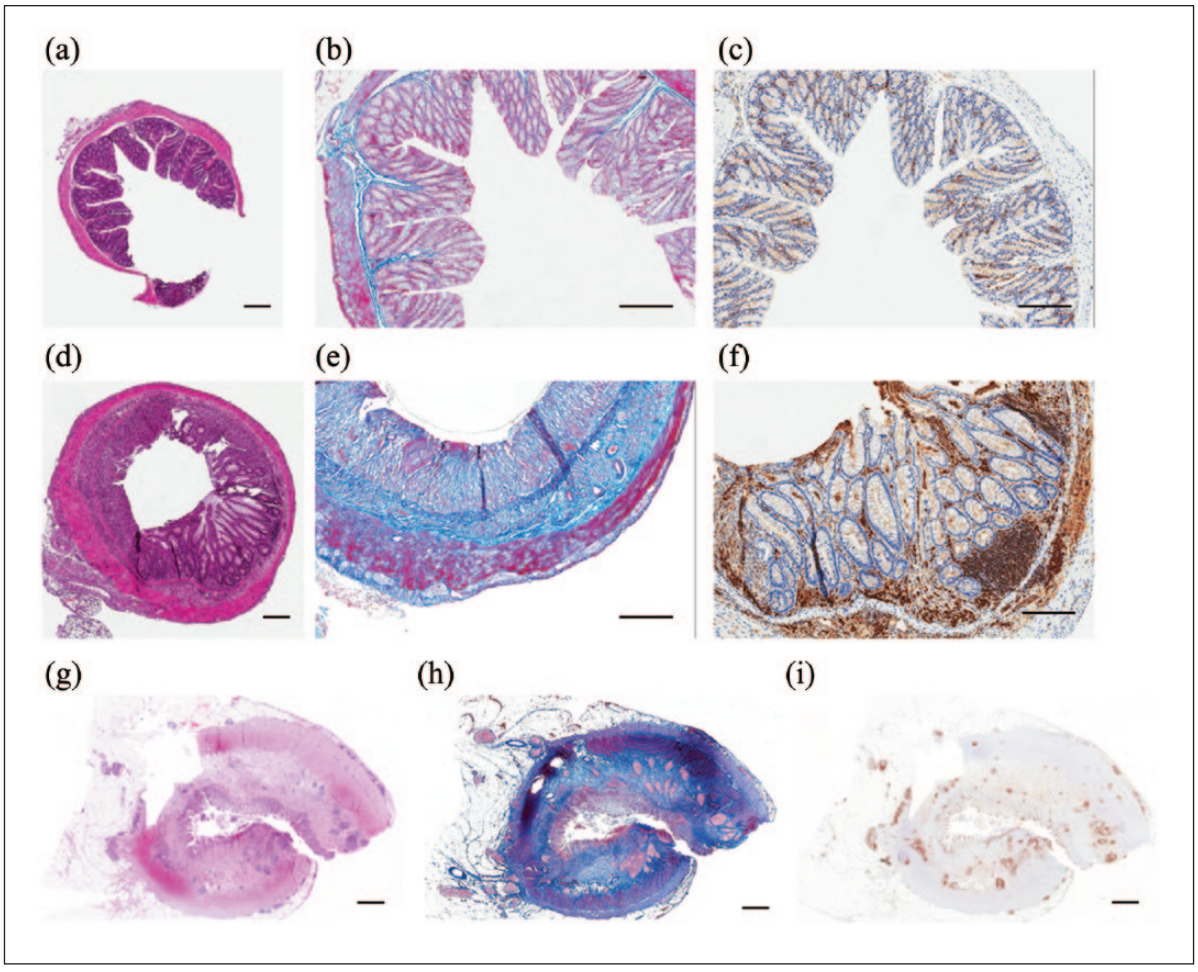

Figure 4. Immune cell infiltration and fibrosis in murine and human colonic samples. H&E staining (a, d, g), Heidenhain's Azan (b, e, g) and IHC staining of infiltrating CD3+ T cells (c, f, i) of untreated (a–c), DSS treated (d–f) and human Crohn's disease patient (g–i). Heidenhain's Azan staining: blue, collagen; pink, nuclei; dark red, cytoplasm. Scale bar: 100 nm.

lymphocytes' infiltration of the lamina propria, while lymphocytes were confined to lymphoid follicles in untreated mice, as expected (Figure 4(f)).

To note, Heidenhain's Azan staining (Figure 4(h)) and IHC of CD3 (Figure 4(i)) of a human Crohn's disease patient confirmed that the quality of the staining of murine samples prepared with the automated system was comparable to those of human samples currently performed in the diagnostic pathology units.

The automated method of sample preparation enhances the reproducibility of histological murine examination

The previous data showed that the application of an automated method generates high-quality murine specimens. In order to assess the practical relevance of this observation, we directly compared the analysis of the same murine samples with a classical manual and with the automated inclusion methods. DSS-treated mice and controls were sacrificed at the end of the experiment, and the colon of each mouse was divided into two equal parts to be processed and included in parallel with the two methods, thus minimizing the inter-sample variations in the evaluation of the parameters. H&E staining was performed, and three sections for each mouse were analysed by a blinded pathologist according to the parameters described in Table 1 (Figure 5).

First, the total number of parameters assessable by the pathologist was calculated for each section (Figure 5(a)–(c)) and normalized for the total number of sections analysed. This experiment confirmed that the preparation of the samples with the automated protocol allowed the assessment of a higher proportion of parameters (and of sections) than the manual method (Figure 5(b) and (c)).

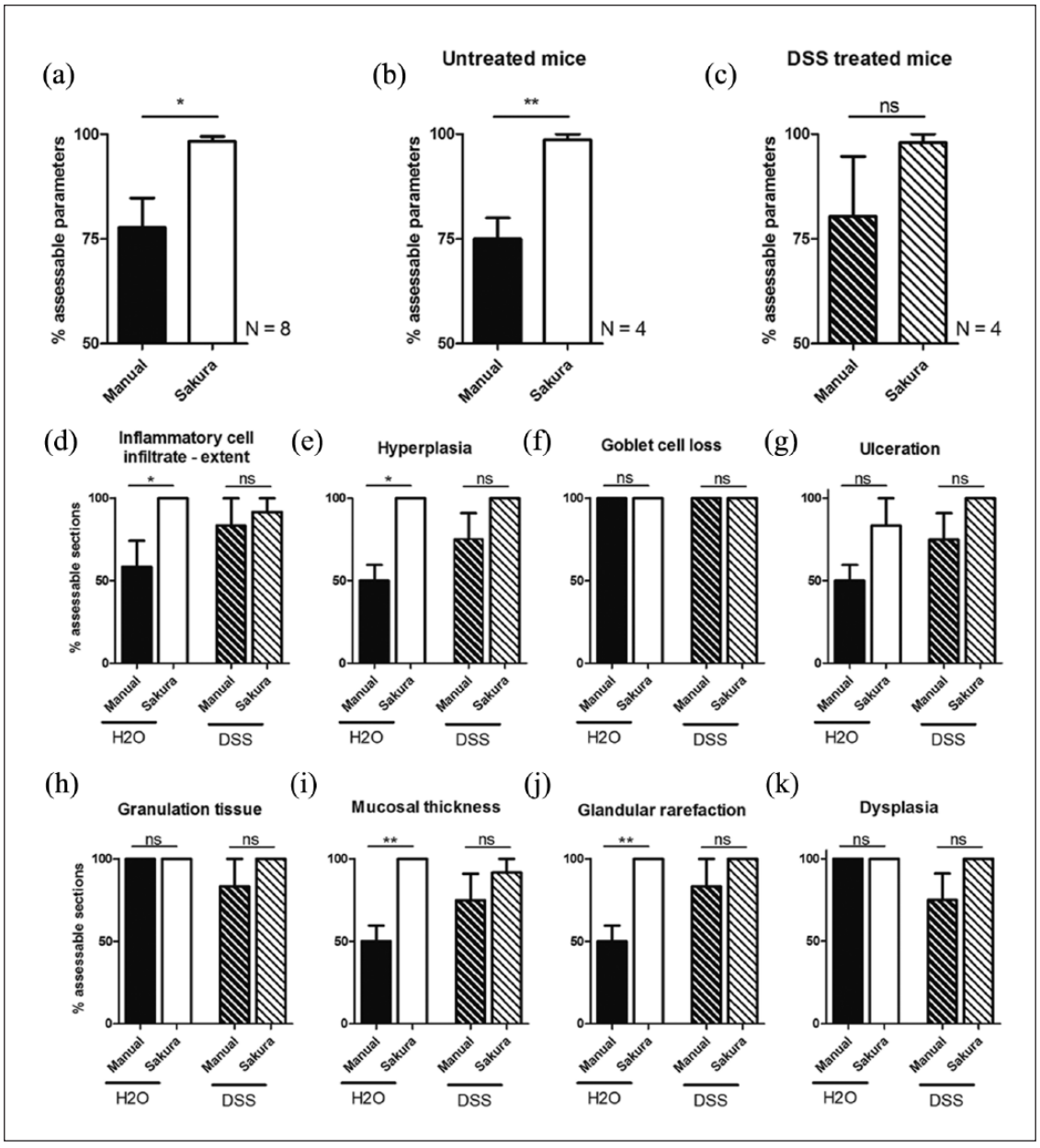

Figure 5. Technical comparison of the histopathologic analyses between manual and automated processing. (a–c) Total percentage of the histopathological parameters accessable by the pathologist in all the sections analysed and prepared with the manual (black bars) or the automated method (white bars), for all the mice evaluated (a, n = 8 mice, three slides per mouse) or divided in healthy controls (b, n = 4, three slides per mouse) and DSS-treated mice (c, n = 4, three slides per mouse). (d–k) Percentage of the sections in which the pathologist was able to estimate each parameter with the manual method (black bars) or with the automated method (white bars) in untreated (plain bars) or DSS-treated mice (striped bars). Statistical significance was calculated using Wilcoxon matched-pairs signed rank t test. *$P < 0.05$; **$P < 0.005$.

To delineate whether the analysis of one or more histological parameters was particularly improved by the automated method, a separate analysis of each item was performed (Figure 5(d)–(k)). A significant difference was observed between manual and automated methods, especially when evaluating the architecture and the basal infiltrate of untreated mice. Interestingly, during DSS-induced intestinal inflammation, differences between the two methods were less pronounced, suggesting that the automated protocol might be superior in detecting subtle variations occurring during milder forms of inflammation.

Discussion

Taken together, our data indicate the applicability of an automated method for sample processing (SAKURA Tissue-Tek automated system) for the analysis of murine intestinal inflammation, used in this context as a feasibility model. The automated method helps in generating high-quality specimens, which can be used to evaluate a broad spectrum of histopathological parameters. Importantly, the automated method demonstrates a significant superiority over manual method for the assessment of the architecture and the basal immune infiltrate of murine colonic tissues.

The necessity to rigorously standardize the histological analysis of murine samples is clearly observed for experimental models of intestinal inflammation. As human IBD is extremely heterogeneous from a clinical and pathological point of view, different experimental murine models were developed in the last few years to recapitulate those pathological outcomes,[10,11] although none of them fully recapitulated the biological complexity of human disease.[12] Murine models of intestinal inflammation secondary to exogenous administration of chemical compounds are widely used, due to their handiness and reproducibility. These include murine colitides caused by acute or chronic administration of DSS in the drinking water,[13,14] or by the rectal instillation of haptenated 2,4,6-Trinitrobenzenesulfonic acid (TNBS)[15] and oxazolone.[16]

The biological complexity of murine IBD models is paralleled by the difficulty to carefully evaluate histological data. Unambiguous definition and grading of inflammatory events, including the type and extent of immune cell infiltration, the changes in the epithelial cell morphology and the changes in the mucosal architecture,[10–12,14] are pivotal for a precise assignment of disease severity.

Histopathological evaluation of human IBD samples is performed by professional pathologists who follow the guidelines jointly elaborated by the European Crohn's and Colitis Organization (ECCO) and the European Society of Pathology (ESP).[17] On the other hand, histological grading of murine experimental colitis lacks standardization and mostly relies on the personal experience of a single laboratory or researcher in the evaluation of a particular model of intestinal inflammation. Several attempts to uniform the histological scoring system for IBD mouse models have been done,[18] and numerous histological scores have been published in the last few years,[3,18,19] even if the pathological effects observed are strictly model-specific. For example, chemically driven colitis models strongly affect epithelial cell integrity and mucosal architecture and induce a robust infiltration of immune cells,[14] while adoptive transfer colitis models induce epithelial hyperplasia, crypt loss but less severe mucosal ulcerations.[20]

Interestingly, while human colitides are characterized by the presence of an eosinophilic infiltrate,[21] in our chemically induced colitis model we failed to detect a relevant presence of this cellular subtype.

We here suggested to utilize an automated standardized method of preparation and inclusion of tissues that is commonly used in human pathology core facilities and also for murine tissue sample preparation. Potentially, this method can be implemented in several murine experimental models. One murine model of chronic intestinal inflammation was chosen as feasibility prototypic example of complex histological evaluation of disease severity and alteration of the architecture of the tissue that might greatly profit from an enhanced quality of sample preparation.

Indeed, we observed that the reduction of manual errors (i.e. the orientation of the sample) given by the use of the cassettes with grids, the elimination of the passage of re-opening of the cassette for the embedding, as well as the strict standardization of technical details such as the fixation time strongly increased the reproducibility of the analysis.

By implementing this method, we succeeded to evaluate fibrosis, a complex biological event occurring in Crohn's Disease (CD) patients, which is very often undervalued in murine models different from chronic TNBS.

We demonstrated a superiority of the automated method in evaluating histopathological parameters associated to the alteration of the tissue architecture, especially in untreated mice. The correct evaluation of the mucosal architecture, of the extent of the inflammatory infiltrate and of the area involved in a particular model of intestinal inflammation is dependent on its comparison with a healthy mucosa. Thus, the capacity to correctly evaluate each parameter in untreated mice is pivotal for the final evaluation of the experimental model result.

We think, therefore, that translational researchers working with murine experimental models of human diseases can benefit from the implementation of this system.

Acknowledgements

We thank the Department of Pathology of the IRCCS (Istituto di Ricovero e Cura a Carattere Scientifico) Policlinico Hospital Milan for the support, the IEO (European Institute of Oncology) Animal Facility for the excellent assistance and Professor Maria Rescigno for critical discussions. F.M.C. and C.B. equally contributed to this work. F.M.C., C.B., G.E. and F.G. performed experiments; F.C. recruited CD patients and obtained biological samples; F.C. and S.B. participated in the interpretation of the data; F.F. conceived and coordinated the study, analysed and interpreted data and wrote of the manuscript. All authors read and approved the final manuscript.

Declaration of conflicting interests

The author(s) declared no potential conflicts of interest with respect to the research, authorship, and/or publication of this article.

Funding

This work was supported by Associazione Italiana per la Ricerca sul Cancro (AIRC; Start-Up grant 14378 to F.F.) and by the Italian Ministry of Health Young Researcher Grant of 2013 to F.C.

References

1. Gibson-Corley KN, Hochstedler C, Sturm M et al. (2012) Successful integration of the histology core laboratory in translational research. *Journal of Histotechnology* 35(1): 17–21.
2. Olivier AK, Naumann P, Goeken A et al. (2012) Genetically modified species in research: Opportunities and challenges for the histology core laboratory. *Journal of Histotechnology* 35(2): 63–67.
3. Gibson-Corley KN, Olivier AK and Meyerholz DK (2013) Principles for valid histopathologic scoring in research. *Veterinary Pathology* 50(6): 1007–1115.
4. Stolfi C, Rizzo A, Franzè E et al. (2011) Involvement of interleukin-21 in the regulation of colitis-associated colon cancer. *Journal of Experimental Medicine* 208(11): 2279–2290.
5. Begley CG and Ellis LM (2012) Drug development: Raise standards for preclinical cancer research. *Nature* 483(7391): 531–153.
6. Peters SR (2010) *A Practical Guide to Frozen Section Technique*. New York: Springer, pp. 1–189.
7. Rosai J (2011) *Rosai and Ackerman's Surgical Pathology*, 10th edn. Edinburgh: Elsevier.
8. https://www.sakura.eu/Our-products/item/7/Tissue-Embedding/83/Tissue-Tek-AutoTEC-Automated-Embedder
9. Chassaing B (2014) Dextran sulphate sodium (DSS)-induced colitis in mice. *Current Protocols in Immunology* 104: Unit 15.25.
10. Blumberg RS, Saubermann LJ and Strober W (1999) Animal models of mucosal inflammation and their relation to human inflammatory bowel disease. *Current Opinion in Immunology* 11(6): 648–156.
11. Mizoguchi A (2012) Animal models of inflammatory bowel disease. *Progress in Molecular Biology and Translational Science* 105: 263–320.
12. DeVoss J and Diehl L (2014) Murine models of inflammatory bowel disease (IBD): Challenges of modeling human disease. *Toxicologic Pathology* 42(1): 99–110.
13. Okayasu I, Hatakeyama S, Yamada M et al. (1990) A novel method in the induction of reliable experimental acute and chronic ulcerative colitis in mice. *Gastroenterology* 98(3): 694–702.
14. Wirtz S, Neufert C, Weigmann B et al. (2007) Chemically induced mouse models of intestinal inflammation. *Nature Protocols* 2(3): 541–556.
15. Neurath MF, Fuss I, Kelsall BL et al. (1995) Antibodies to interleukin 12 abrogate established experimental colitis in mice. *Journal of Experimental Medicine* 182(5): 1281–1290.
16. Boirivant M, Fuss IJ, Chu A et al. (1998) Oxazolone colitis: A murine model of T helper cell type 2 colitis treatable with antibodies to interleukin 4. *Journal of Experimental Medicine* 188(10): 1929–1939.
17. Magro F, Langner C, Driessen A et al. (2013) European consensus on the histopathology of inflammatory bowel disease. *Journal of Crohn's and Colitis* 7(10): 827–851.
18. Erben U, Loddenkemper C, Doerfel K et al. (2014) A guide to histomorphological evaluation of intestinal inflammation in mouse models. *International Journal of Clinical and Experimental Pathology* 7(8): 4557–4576.
19. Kozlowski C, Jeet S, Beyer J et al. (2013) An entirely automated method to score DSS-induced colitis in mice by digital image analysis of pathology slides. *Disease Models & Mechanisms* 6(3): 855–865.
20. Powrie F, Leach MW, Mauze S et al. (1994) Inhibition of Th1 responses prevents inflammatory bowel disease in scid mice reconstituted with CD45RBhi CD4+ T cells. *Immunity* 1(7): 553–562.
21. Villanacci V, Antonelli E, Reboldi G et al. (2014) Endoscopic biopsy samples of naive 'colitides' patients: Role of basal plasmacytosis. *Journal of Crohn's and Colitis* 8(11): 1438–1443.